



**FULL PAPER**

Applied  
Organometallic  
Chemistry

**WILEY**

# A series of Salen-type homodinuclear lanthanide complexes and their slow magnetic relaxation in Dy<sub>2</sub> and Ho<sub>2</sub>

Lun Zhang<sup>1</sup> | Pei-Pei Yang<sup>1,2</sup> | Ling-Fei Li<sup>1</sup> | Yi-Ye Hu<sup>1</sup> | Yu Gao<sup>1</sup> | Jin Tao<sup>3</sup>

<sup>1</sup>College of Chemistry and Materials Science, Huaibei Normal University, 100 Dongshan Road, Huaibei, 235000, People's Republic of China

<sup>2</sup>Anhui Key Laboratory of Energetic Materials, Huaibei Normal University, 100 Dongshan Road, Huaibei, 235000, People's Republic of China

<sup>3</sup>Jiangsu Key Laboratory for NSLSCS, School of Physical Science and Technology, Nanjing Normal University, Nanjing, 210023, People's Republic of China

Pei-Pei Yang, College of Chemistry and Materials Science, Huaibei Normal University, 100 Dongshan Road, Huaibei, 235000, People's Republic of China.  
Email: hbnuypp@163.com

Jin Tao, Jiangsu Key Laboratory for NSLSCS, School of Physical Science and Technology, Nanjing Normal University, Nanjing 210023, People's Republic of China.  
Email: taojin1@njnu.edu.cn

## Funding information

Foundation for Young Talents in College of Anhui Province, Grant/Award Numbers: no. gxyqZD2016412, gxyqZD2016412; Anhui Provincial Innovation Team of Design and Application of Advanced Energetic Materials, Grant/Award Number: KJ2015TD003

A series of homodinuclear lanthanide complexes, namely,  $[\text{Ln}_2(\text{L})_2(\text{MeOH})_2(\text{NO}_3)_2]$  [ $\text{Ln} = \text{Gd}$  (**1**),  $\text{Tb}$  (**2**),  $\text{Dy}$  (**3**), and  $\text{Ho}$  (**4**)], were synthesized by the reaction of Salen-type ligand, namely *N,N'*-bis(5-bromosalicylidene)ethane-1,2-diamine ( $\text{H}_2\text{L}$ ), with lanthanide salts in methanol and acetonitrile solution. The two  $\text{Ln}^{\text{III}}$  ions in **1–4** are linked by two  $\text{O}_{\text{phenoxo}}$  atoms of two  $\text{L}^{2-}$  ligands to build a dinuclear skeleton. The eight-coordinate  $\text{Ln}^{\text{III}}$  center adopts a triangular dodecahedron geometry of  $D_{2\text{d}}$  symmetry. Theoretical calculations revealed that antiferromagnetic interactions exist in those complexes. Dynamic magnetic properties studies indicate that the  $\text{Dy}_2$  complex behaves as a single-molecule magnet with an anisotropy barrier of  $U_{\text{eff}} \approx 47.68$  K and a pre-exponential factor  $\tau_0 = 3.17 \times 10^{-6}$  s under a zero applied field, whereas the  $\text{Ho}_2$  complex exhibits a fast tunneling relaxation process that is rationalized through *ab initio* calculations.

## KEY WORDS

antiferromagnetic interactions, homodinuclear lanthanide complexes, Salen-type ligand, single-molecule magnet

## 1 | INTRODUCTION

Single-molecule magnets (SMMs) have attracted much attention because of their potential applications in high-density information storage, magnetic refrigerators, and quantum computing.<sup>[1]</sup> SMMs are discrete molecular

complexes that show slow relaxation in the absence of an external magnetic field and hysteresis loops because of the presence of an energy barrier to the magnetization reversal.<sup>[2]</sup> Since the discovery of mononuclear lanthanide complexes exhibiting fascinating properties,<sup>[3]</sup> sustained efforts have been focused on developing

lanthanide-based SMMs (Ln-SMMs).<sup>[4]</sup> In comparison with transition elements, lanthanide ions provide large magnetic moments and significant intrinsic magnetic anisotropies profiting from a strong spin-orbit coupling effect, making them ideal candidates for the construction of high-performance SMMs.<sup>[5]</sup> Especially the Dy<sup>III</sup> ion, arising from its bistable nature of the ground state irrespective of the ligand field, significant magnetic anisotropy, and large magnetic moment,<sup>[6]</sup> has indisputably yielded the largest quality of strongly blocked Ln-SMMs.

Notably, lanthanide complexes of low nuclearity (mononuclear in particular) should be better SMMs.<sup>[7]</sup> Indeed, the dysprosium metallocene cation reported by Layfield and co-workers very recently showed a new record energy barrier ( $U_{\text{eff}} = 2217$  K) and blocking temperature ( $T_B = 80$  K), which represents the best SMM reported to date.<sup>[8]</sup> Compared with mononuclear lanthanide complexes, dinuclear lanthanide complexes have been regarded as the simplest molecular unit, which allows to easily understand in-depth the nature and strength of magnetic coupling between two spin carriers and finally reveal the magnetic relaxation mechanism affected by magnetic interaction. However, those have been only little explored in lanthanide systems,<sup>[9–11]</sup> particularly in anisotropic lanthanides.<sup>[11]</sup> Moreover, the use of *ab initio* calculation and electrostatic analysis to explore the SMM properties of rare earth metal complexes (such as anisotropic energy barriers [ $U_{\text{eff}}$ ]) is also a hot topic in molecular magnetics.<sup>[12]</sup> In a number of dilanthanide complexes, magnetic exchange interactions have been also modelled by *ab initio* calculations.<sup>[13]</sup>

Clearly, it remains a significant challenge to establish rational and effective guidelines for synthesizing dinuclear Ln-SMMs, exploring the effect of *f-f* interactions and uniaxial anisotropy on magnetic behavior. It has been reported that the magnetic anisotropy for Ln-SMMs is extremely sensitive to the ligand field effects and the coordination geometry of the lanthanide metal ion.<sup>[14]</sup> Therefore, choosing the suitable organic ligand is necessary for the preparation of dinuclear Ln-SMMs. According to the literature research, the ligands utilized in the preparation of dinuclear lanthanide complexes are comparatively few and limited to the Schiff bases obtained from *o*-vanillin or its derivatives, with different kinds of amines.<sup>[15–17]</sup> As a special Schiff base, the Salen ligands, which are condensation products from salicylaldehyde and diamine, exhibit good coordination ability, and hence have been used for constructions of functional coordination complexes. Compared with the amount of effort on the 3d–4f heteronuclear complexes from Salen-type Schiff base ligands,<sup>[18]</sup> the pure polynuclear lanthanide Salen complexes (especially for

dinuclear complexes) have not been researched nearly as extensively.<sup>[19]</sup> With the aim to extend the search for new dinuclear lanthanide complexes, a Salen-type ligand, namely, *N,N'*-bis(5-bromosalicylidene)-ethane-1,2-diamine ( $H_2L$ ), was chosen to react with lanthanide salts. Thus, in this paper, we report the structures and magnetic properties of a family of dinuclear Ln<sup>III</sup> complexes obtained from the  $H_2L$  ligand, namely,  $[\text{Ln}_2(L)_2(\text{MeOH})_2(\text{NO}_3)_2]$ , where  $\text{Ln} = \text{Gd}$  (**1**),  $\text{Tb}$  (**2**),  $\text{Dy}$  (**3**),  $\text{Ho}$  (**4**). Magnetic studies indicate that there are anti-ferromagnetic interactions between the Ln<sup>3+</sup> ions in those complexes. Complexes **3** and **4** exhibit a slow magnetic relaxation and complex **3** has an anisotropy barrier of  $U_{\text{eff}} \approx 47.68$  K and a pre-exponential factor  $\tau_0 = 3.17 \times 10^{-6}$  s. The uniaxial magnetic anisotropies and relaxation mechanism of complexes **3** and **4** were investigated in depth by *ab initio* calculations.

## 2 | EXPERIMENTAL

### 2.1 | Syntheses and infrared spectra for complexes 1–4

Triethylamine (0.0101 g, 0.1 mmol) was added dropwise to a 10 mL solution of methanol and acetonitrile (1:1) containing  $\text{Ln}(\text{NO}_3)_3 \cdot 6\text{H}_2\text{O}$  (0.1 mmol) and  $H_2L$  (0.0426 g, 0.1 mmol). After that, the mixture was stirred at room temperature for 0.5 hr. The mixture was then transferred to a 25-mL Teflon-lined autoclave, and heated at 80 °C in a precision thermostatic blast oven. After 5 days, it was cooled to 30 °C at a rate of 5 °C every 2 hr. Yellow crystals suitable for X-ray diffraction were collected and washed three to five times with cold MeOH in a yield of 35%–40%. The complexes were characterized by elemental analysis and Fourier-transform infrared (FT-IR). The characteristic data of these complexes are as follows:

$[\text{Gd}_2(L)_2(\text{MeOH})_2(\text{NO}_3)_2]$  (**1**): Elemental analyses (%), calculated: C 30.22, H 2.36, N 6.23. Found: C 30.20, H 2.37, N 6.22. IR (KBr) ( $\text{cm}^{-1}$ ): 3831 (m), 3743 (m), 3674 (m), 3390 (m), 2982 (m), 2354 (m), 1625 (w), 1464 (w), 1382 (w), 1314 (w), 1267(m), 1173 (m), 1014 (m), 828 (m), 691 (m), 635 (m), 440 (w).

$[\text{Tb}_2(L)_2(\text{MeOH})_2(\text{NO}_3)_2]$  (**2**): Elemental analyses (%), calculated: C 30.12, H 2.34, N 6.22. Found: C 30.13, H 2.36, N 6.20. IR (KBr) ( $\text{cm}^{-1}$ ): 3851 (m), 3749 (m), 3648 (m), 3402 (m), 2926 (m), 2381 (m), 1626 (w), 1465 (w), 1383 (w), 1314 (w), 1268 (w), 1173 (m), 1012 (m), 827 (m), 690 (m), 634 (m), 442 (s).

$[\text{Dy}_2(L)_2(\text{MeOH})_2(\text{NO}_3)_2]$  (**3**): Elemental analyses (%), calculated: C 29.98, H 2.34, N 6.17. Found C 29.97, H 2.35,

N 6.17. IR (KBr) ( $\text{cm}^{-1}$ ): 3851 (m), 3749 (m), 3647 (m), 3419 (m), 2894 (s), 2359 (m), 1627 (w), 1466 (w), 1383 (w), 1314 (w), 1269 (m), 1174 (m), 1014 (m), 828 (m), 691 (m), 635 (s), 443 (s).

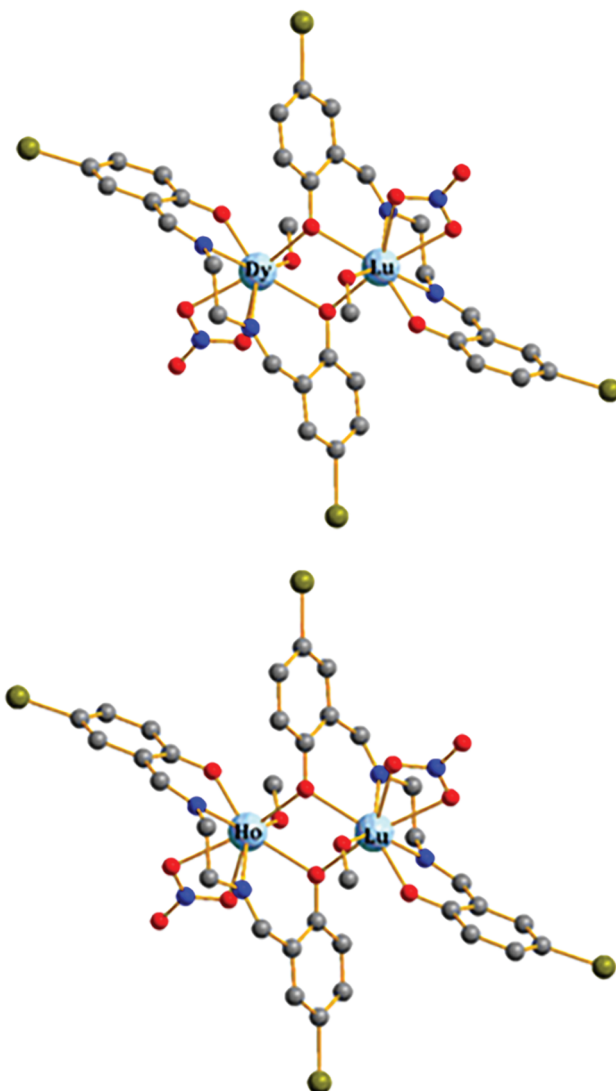
[Ho<sub>2</sub>(L)<sub>2</sub>(MeOH)<sub>2</sub>(NO<sub>3</sub>)<sub>2</sub>] (**4**): Elemental analyses (%), calculated: C 29.87, H 2.35, N 6.14. Found: C 29.86, H 2.34, N 6.15. IR (KBr) ( $\text{cm}^{-1}$ ): 3853 (m), 3752 (m), 3650 (m), 3394 (m), 2942 (m), 2365 (m), 1628 (m), 1465 (m), 1383 (m), 1315 (m), 1268 (m), 1172 (m), 1012 (m), 827 (m), 688 (m), 635 (m), 439 (s).

## 2.2 | Materials and physical measurements

All reagents used in the experiment were of analytical reagent grade. All reagents were obtained from commercial sources and used without further purification. The Schiff base ligand, *N,N'*-bis(5-bromosalicylidene)ethane-1,2-diamine (H<sub>2</sub>L) (Scheme 1a), was synthesized by condensation of 5-bromosalicylaldehyde and ethylenediamine in a 2:1 aqueous ethanol solution, according to the experimental methods mentioned in the literature.<sup>[20]</sup> Elemental analyses (C, H, and N) were performed using an Elementar Vario EL analyzer. IR spectra were measured on a Bruker Tensor 27 spectrometer with samples prepared as KBr disks. The magnetic properties were measured on an MPMS SQUID VSM magnetometer. Alternating current (AC) susceptibility measurements were performed with an oscillating AC field of 2.0 Oe and AC frequencies ranging from 1 to 1000 Hz.

## 2.3 | X-ray structure determinations

The crystal data for complexes **1–4** were collected on a Rigaku Saturn CCD diffractometer using graphite-monochromated Cu-K $\alpha$  radiation ( $\lambda = 1.54184 \text{ \AA}$ ) at 293 K. Crystal field data gathering ( $\omega$  scan) and processing were carried out using the Crystal Clear Pack (Cell Refinement, Data Simplification and Empirical Absorption Correction).<sup>[21]</sup> All structures were solved by direct methods and refined by full-matrix least-squares methods of  $F^2$  using the shelxl97 package. All non-hydrogen atoms were refined anisotropically.<sup>[22]</sup> The positions of the rare earth metal atoms were easily determined, and the O, N, and C atoms were then determined by the differential Fourier map. The hydrogen atoms were introduced to calculated positions as riding on their respective bonded atoms. Crystal data and structural refinements are listed in Table URE S1. CCDC (Cambridge Crystallographic Data Centre) 1904959 (**1**), 1904960 (**2**), 1904961 (**3**), 1904962 (**4**) contain all supplementary crystallographic data of these four complexes.



**SCHEME 1** (a) Structure of the H<sub>2</sub>L ligand; (b) coordination mode of the L<sup>2-</sup> ligand

## 3 | RESULTS AND DISCUSSION

### 3.1 | Syntheses and IR spectra

Ln(NO<sub>3</sub>)<sub>3</sub>·6H<sub>2</sub>O was reacted with H<sub>2</sub>L (Scheme 1a) and triethylamine in a ratio of 1:1:1 in a solvent of MeOH and MeCN to obtain a series of dinuclear lanthanide complexes. As the normal temperature method does not give us the desired product, we synthesized complexes **1–4** by the solvothermal method. The IR spectrum of complexes **1–4** show all of the characteristic bands of the coordinated ligand L<sup>2-</sup>. Because of  $\nu(\text{C}=\text{N})$  stretching, one such protruding band appeared at about 1625 cm<sup>-1</sup>, and the characteristic band caused by  $\nu(\text{C}-\text{O})$  appears at about 1269 cm<sup>-1</sup>. For NO<sub>3</sub><sup>-</sup> anions, characteristic bands appear around 1380 cm<sup>-1</sup> as expected.<sup>[23]</sup> The phase purities of the as-synthesized complexes **1–4** were demonstrated by

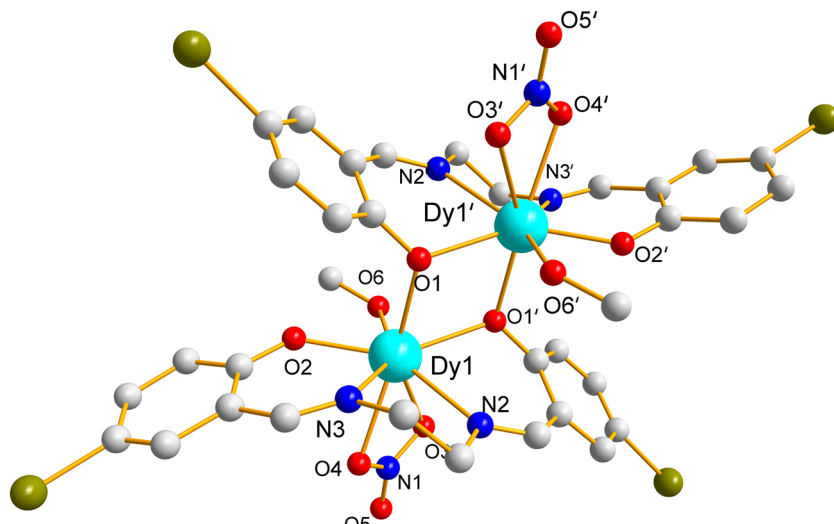


**FIGURE 1** Molecular structure of complex 3. H atoms are omitted for clarity

X-ray powder diffraction. As shown in Figures S7–S10, all experimental peaks are in agreement with those in the simulated profile derived from single-crystal diffraction data, which demonstrates the high phase purity of the four complexes.

### 3.2 | Description of the structures

The single-crystal X-ray diffraction studies confirmed that complexes **1**–**4** are isostructural and crystallize in the triclinic space group  $P^1$  (**Table** URE S1). The molecular structure of complexes **1**, **2**, and **4** and coordination environments for the  $\text{Ln}^{III}$  ion in complexes **1**, **2**, and **4** are shown in Figures URE S1–S6. Here, for the sake of convenience, the crystal structure of complex **3** is elaborated as a representative. As shown in Figure 1, each asymmetric unit of complex **3** contains two  $\text{Dy}^{III}$  ions, two  $\text{L}^{2-}$  ligands, two nitrate ions, and two neutral methanol ligands. The  $\text{L}^{2-}$  ligand adopts the  $\eta^1:\eta^1:\eta^1:\eta^2:\mu^2$  coordination mode (Scheme 1b). The two  $\text{Dy}^{III}$  ions are bridged by two  $\text{O}_{\text{phenoxo}}$  atoms ( $\text{O}_1$ ,  $\text{O}'_1$ ) from two  $\text{L}^{2-}$  ligands to form a dimer. Each  $\text{Dy}^{III}$  ion has an eight-coordinate environment composed of two nitrogen atoms ( $\text{N}_2$  and  $\text{N}_3$ ) and three oxygen atoms ( $\text{O}_1$ ,  $\text{O}'_1$ , and  $\text{O}_2$ ) from two  $\text{L}^{2-}$  ligands, two oxygen atoms ( $\text{O}_3$  and  $\text{O}_4$ ) from a nitrate ion, and one oxygen atom ( $\text{O}_6$ ) from a methanol molecule. The  $\text{Dy}-\text{N}$  bond lengths are in the range of 2.471(5)–2.932(6) Å, and the  $\text{Dy}-\text{O}$  bond distances are 2.166(11)–2.514(11) Å. The bond angles of  $\text{O}_1-\text{Dy}_1-\text{O}'_1$ ,  $\text{O}_1-\text{Dy}_1'-\text{O}'_1$  were 70.20(4)° (**Table** S2). These bond lengths and angles are consistent with the reported data.<sup>[24]</sup> To determine the local coordination environment symmetry of the eight-coordinated  $\text{Dy}^{III}$  ions, the continuous shape measure parameters of the  $\text{Dy}^{III}$  centers were analyzed (**Table** S3) using the Shape 2.1 software,<sup>[25]</sup> which indicated a symmetry closest to a

triangular dodecahedron geometry of  $D_{2d}$  (as shown in Figure 2). The intramolecular  $\text{Dy}\cdots\text{Dy}$  distance is 3.816 (16) Å, suggesting the potential interaction between  $\text{Dy}^{III}$  ions. The shortest  $\text{Dy}\cdots\text{Dy}$  distance between the adjacent dinuclear molecules is 7.082(14) Å.

### 3.3 | Magnetic properties

#### 3.3.1 | Static susceptibility measurements

Variable-temperature (2–300 K) direct current (DC) magnetic susceptibilities for all complexes were measured on crystal samples under an applied DC magnetic field of 1 kOe. After the data processing,

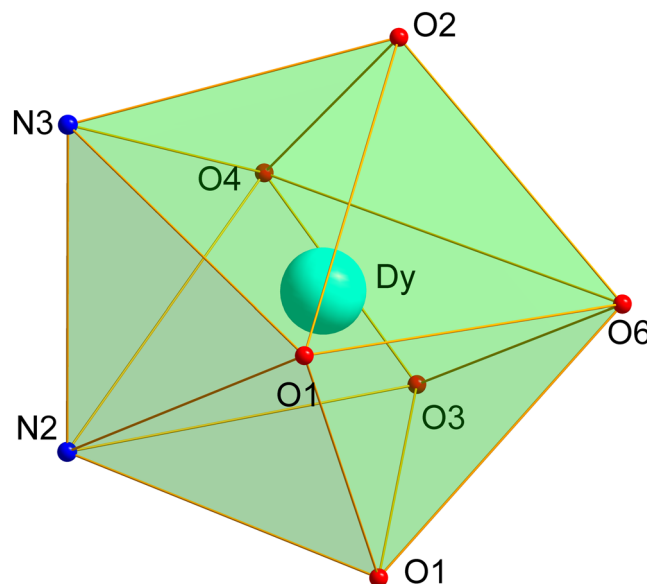


**FIGURE 2** Coordination environment for the  $\text{Dy}^{III}$  ion in complex 3

variable-temperature magnetic-susceptibility curves were obtained, as shown in Figure 3. For complexes **1** and **2**, at 300 K, the experimental  $\chi_M T$  values of 15.79 and 23.53 cm<sup>3</sup> K mol<sup>-1</sup> are in good agreement with the theoretical values of two uncoupled Gd<sup>3+</sup> ions (<sup>8</sup>S<sub>7/2</sub>,  $S = 7/2$ ,  $L = 0$ ,  $g = 2$ ,  $C = 15.76$  cm<sup>3</sup> K mol<sup>-1</sup>) and Tb<sup>3+</sup> ions (<sup>7</sup>F<sub>6</sub>,  $S = 3$ ,  $L = 3$ ,  $g = 3/2$ ,  $C = 23.64$  cm<sup>3</sup> K mol<sup>-1</sup>), respectively. For complexes **3** and **4**, at room temperature, the experimental  $\chi_M T$  values are 27.30 and 27.92 cm<sup>3</sup> K mol<sup>-1</sup>, which are slightly smaller than the expected values of two uncoupled Dy<sup>3+</sup> ions (<sup>6</sup>H<sub>15/2</sub>,  $S = 5/2$ ,  $L = 5$ ,  $g = 4/3$ ,  $C = 28.34$  cm<sup>3</sup> K mol<sup>-1</sup>), and Ho<sup>3+</sup> ions (<sup>5</sup>I<sub>8</sub>,  $S = 2$ ,  $L = 6$ ,  $g = 5/4$ ,  $C = 28.14$  cm<sup>3</sup> K mol<sup>-1</sup>), respectively.<sup>[26]</sup> Upon cooling, the  $\chi_M T$  values of complexes **1–4** gradually decrease to 14.64, 21.73, 24.77, 25.32 cm<sup>3</sup> K mol<sup>-1</sup> at 70 K. With further cooling,

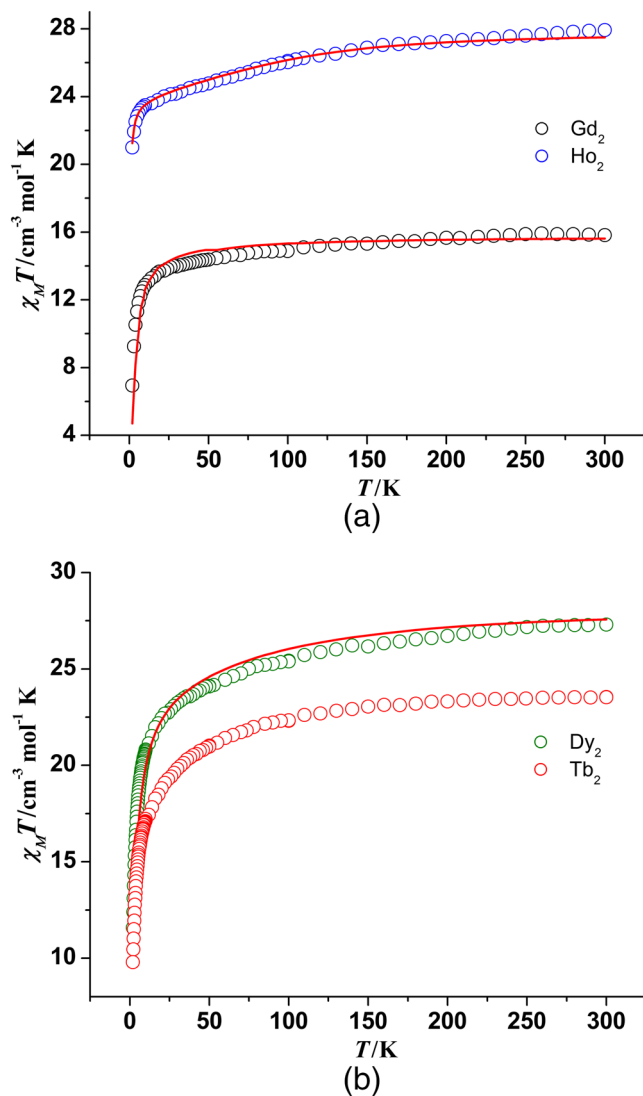


**FIGURE 3** (a) Plots of  $\chi_M T$  versus  $T$  under a magnetic field of 1 kOe for complexes Gd<sub>2</sub> and Ho<sub>2</sub>. (b) Plots of  $\chi_M T$  versus  $T$  under a magnetic field of 1 kOe for complexes Tb<sub>2</sub> and Dy<sub>2</sub>. The red solid line represents the result of *ab initio* calculations

the  $\chi_M T$  values of complexes **1–4** are drastically reduced. Their  $\chi_M T$  reach the deepest values of 6.93, 9.80, 11.58, 21.01 cm<sup>3</sup> K mol<sup>-1</sup> at 2 K, respectively. Given that the anisotropy of Gd<sup>III</sup> is negligible, the behavior of complex **1** is consistent with the presence of weak intramolecular antiferromagnetic exchange interactions.<sup>[27]</sup> For complexes **2–4**, such performance can be assigned to antiferromagnetic coupling and/or the progressive thermal depopulation of the excited Stark sublevels of the Ln<sup>III</sup> ions.<sup>[28]</sup>

The field-dependent magnetization ( $M$ ) of complexes **1–4** were measured at a temperature of 2 K and the magnetic field strength was in the range of 0–70 KOe. As shown in Figures 4 and S11, the saturation susceptibility  $M$  value for the two Gd<sup>3+</sup> ions ( $S = 7/2$ ) in complex **1** was 13.78  $N\beta$ , which is close to the expected saturation value of 14  $N\beta$  for two isolated Gd<sup>3+</sup> ions. The corresponding magnetization data can be well fitted via the Brillouin function, as shown in Figure 4. The presence of the Brillouin function for magnetically uncoupled Gd<sup>III</sup> ions is above the experimental magnetization curve ( $S = 7/2$ ,  $g = 2.0$ ), further revealing the antiferromagnetic exchange interactions in the dinuclear Gd complex.<sup>[29]</sup> For anisotropic complexes **2–4**, the field-dependent magnetization shows a rapid increase at low field followed by a slow linear increase at high field with maxima of 9.62  $N\beta$  (**2**), 10.39  $N\beta$  (**3**), and 11.16  $N\beta$  (**4**), under 7 T without reaching the corresponding theoretical saturation values (18  $N\beta$  for two Tb<sup>3+</sup> ions, 20  $N\beta$  for two isolated Dy<sup>3+</sup> ions, and 20  $N\beta$  for two Ho<sup>3+</sup> ions, respectively),<sup>[30]</sup> which is indicative of the presence of significant magnetic anisotropy and/or low-lying excited states.

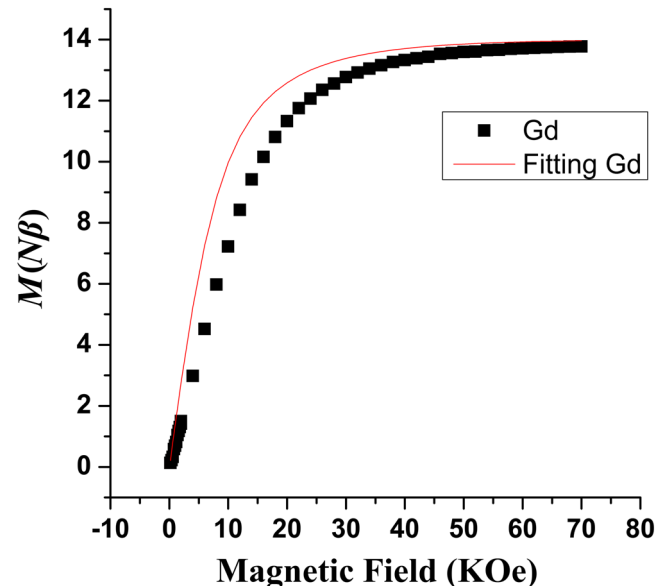


**FIGURE 4** Field dependence of magnetization at 2.0 K in the field range of 0–70 kOe for complex **1**. Brillouin functions for magnetically uncoupled Gd<sup>III</sup> ions (red line)

### 3.3.2 | Dynamic magnetic properties

To further investigate the magnetic kinetics of complexes **2–4**, the temperature and frequency dependence of the AC susceptibility was measured under a zero DC field with an alternating magnetic field of 2 Oe oscillating in the range of 100–1000 Hz. At  $H_{dc} = 0$  Oe, unfortunately, complex **2** (Figure 5) does not exhibit frequency dependence; instead, only complexes **3** (Figure 6) and

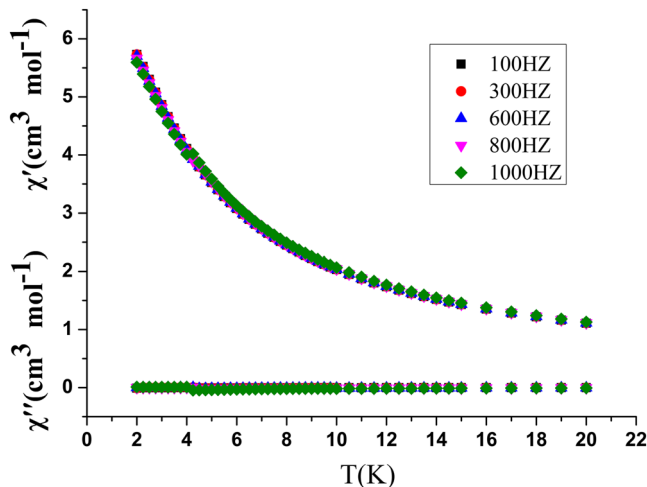


**FIGURE 5** Temperature dependence of the in-phase ( $\chi'$ ) and out-of-phase ( $\chi''$ ) AC susceptibilities of complex **2** under a zero DC field with an oscillating field of 2 Oe in the frequency range of 100–1000 Hz

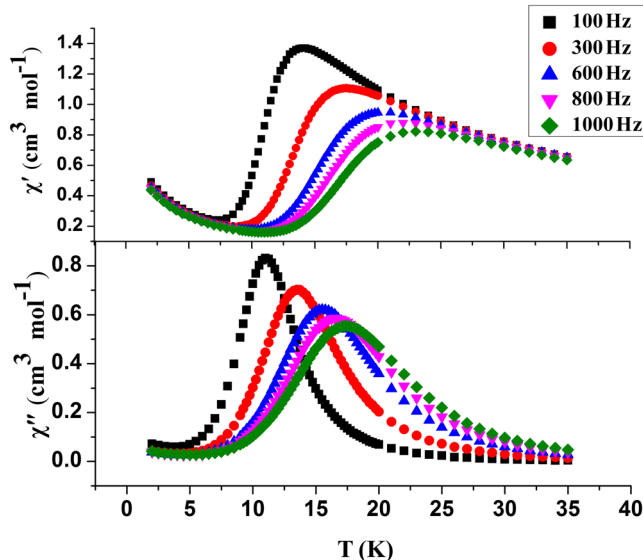


**FIGURE 6** Temperature dependence of the in-phase ( $\chi'$ ) and out-of-phase ( $\chi''$ ) AC susceptibilities of complex **3** under a zero DC field with an oscillating field of 2 Oe in the frequency range of 100–1000 Hz

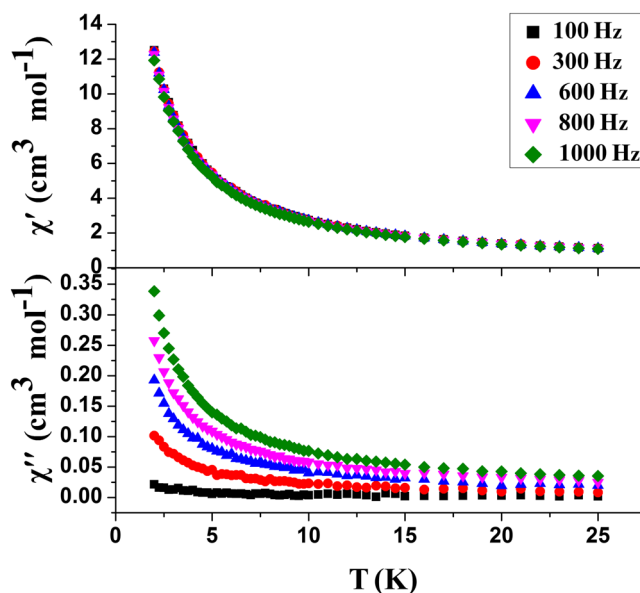


**FIGURE 7** Temperature dependence of the out-of-phase ( $\chi''$ ) AC susceptibilities of complex **4** under a zero DC field with an oscillating field of 2 Oe in the frequency range of 100–1000 Hz

**4** (Figure 7) exhibit strong temperature- and frequency-dependent in-phase ( $\chi'$ ) and out-of-phase ( $\chi''$ ) AC susceptibility signals, confirming the SMM nature for complexes **3** and **4**.<sup>[20]</sup> However, no  $\chi''$  signal peaks for complex **4** can be found in the available frequency range until 2.0 K, which may be attributed to the fast quantum tunneling relaxation.

For complex **3**, as shown in Figure 6, variable-temperature  $\chi'$  and  $\chi''$  data are not only frequency dependent (below 25 K) but also exhibit sharp maxima in the ranges 14.25–23 K and 11.00–17.50 K, respectively. Furthermore, the dynamics of the magnetization of complex **3** have been studied by measuring its frequency dependencies on the AC susceptibility under a zero DC field. As shown in Figure 8, the in-phase ( $\chi'$ ) and out-of-phase ( $\chi''$ ) signals of complex **3** show strong frequency dependencies, suggesting the presence of slow magnetic relaxation. The relaxation times ( $\tau$ ) extracted from the  $\chi''$  peaks for complex **3** at selected temperatures were used to construct the Arrhenius plot<sup>[31]</sup> shown in Figure 9. For complex **3**,  $\ln(\tau)$  versus  $T^{-1}$  plots were fitted to provide an anisotropy barrier of  $U_{eff} \approx 47.68$  K with a pre-exponential factor ( $\tau_0$ ) of  $3.17 \times 10^{-6}$  s (theoretical value  $\tau_0 = 10^{-6}$ – $10^{-11}$  s).<sup>[32]</sup> Besides, the Cole–Cole plots based on the frequency-dependent AC magnetic-susceptibility measurement in the temperature range of 8.0–20 K (Figure 10) reveal an asymmetrical semicircular shape. These data can be fitted with generalized Debye model<sup>[33]</sup> to give values of  $\alpha$  parameter in the range of 0.09–0.23, which indicates a relatively narrow width of relaxation processes most likely due to a combination of quantum

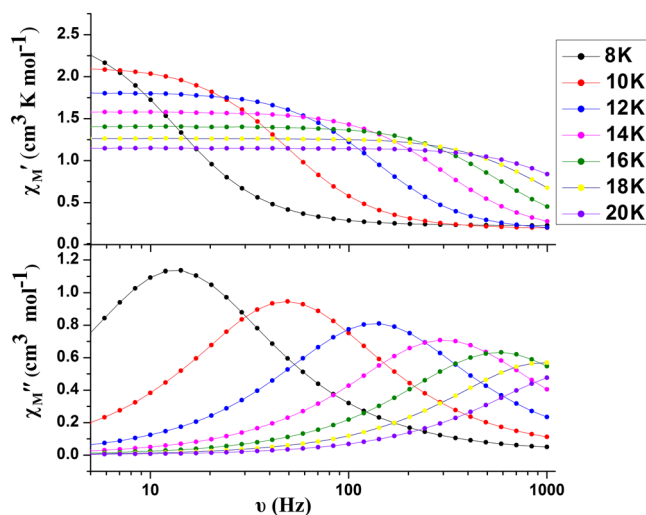


**FIGURE 8** Frequency dependence of the in-phase ( $\chi' M'$ ) and out-of-phase ( $\chi'' M''$ ) products under zero DC field for complex 3

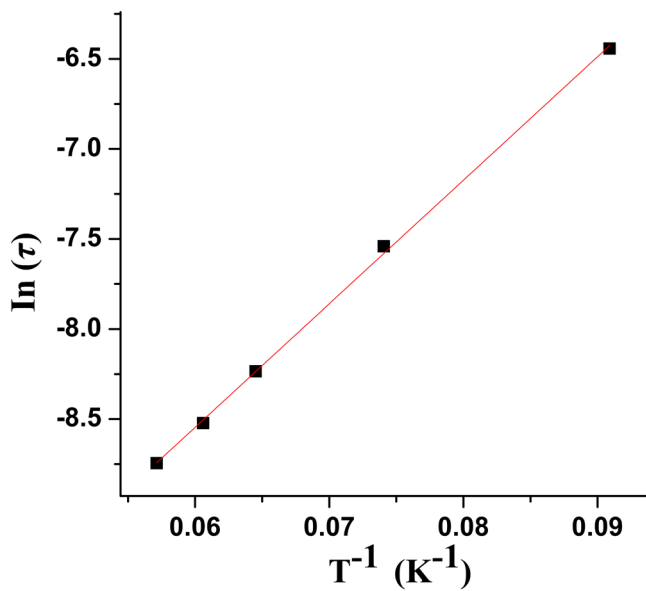


**FIGURE 9** Plot of  $\ln(\tau)$  versus  $T^{-1}$  fitting to the Arrhenius law for complex 3

tunneling of magnetization (QTM) and thermally assisted relaxation pathways.[13a, 34a]

To date, some Salen-type binuclear Dy<sup>III</sup><sub>2</sub> SMMs with similar ligands have been reported. For comparison with previously reported analogs, the relevant parameters are given in Table 1. Complex 3 shows a comparatively higher  $U_{\text{eff}}$  among the pure Salen-type dinuclear dysprosium SMMs. Furthermore, replacing hydrogen atoms with electron-withdrawing atoms on the terminal Salen-type ligands could be a comparatively straightforward way of attaining larger barriers ( $U_{\text{eff}}$ ), such as complex 3, [Dy<sub>2</sub>(valdien)<sub>2</sub>(ClCH<sub>2</sub>OO)<sub>2</sub>], [Dy<sub>2</sub>(valdien)<sub>2</sub>(Cl<sub>2</sub>CH

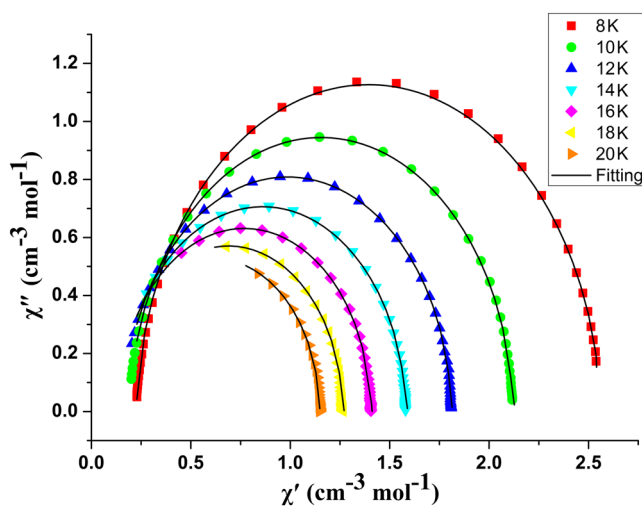


**FIGURE 10** Cole–Cole plot of complex 3 at temperatures between 8.0 and 20 K. The solid lines are fits of the experimental data using a generalized Debye model

[COO)<sub>2</sub>]·0.5CH<sub>3</sub>OH, [Dy<sub>2</sub>(valdien)<sub>2</sub>](CF<sub>3</sub>COCHCOCF<sub>3</sub>)<sub>2</sub>], [13a], and [Dy<sub>2</sub>(valdien)<sub>2</sub>(NO<sub>3</sub>)<sub>2</sub>].[34b]

For complex 4, to suppress the stronger QTM, AC measurements were performed at 2.0 K with 2000 Oe applied DC fields in the frequency range of 100–1000 Hz on complex 4 (Figure S12). Unfortunately, the out-of-phase ( $\chi''$ ) AC susceptibility exhibits clear frequency dependence, but still no frequency-dependence peaks were found, which indicates that QTM is not suppressed. Thus, profiles exclude the calculation of  $U_{\text{eff}}$  for complex 4. But here, it must be noted that complex 4 is a rare phenoxy-O-bridged Ho<sub>2</sub>-Salen-type complex with slow magnetic relaxation behavior. To the best of our knowledge, only one case of a phenoxy-O-bridged Ho<sub>2</sub> complex, namely, [Ho<sub>2</sub>L'<sub>2</sub>(NO<sub>3</sub>)<sub>2</sub>(C<sub>2</sub>H<sub>5</sub>OH)<sub>2</sub>]0.5py, where H<sub>2</sub>L' = 2-{[(2-hydroxy-3-methoxy benzyl)imino]methyl} naphtha-len-1-ol<sup>[35]</sup> showed slow magnetic relaxation ).

### 3.3.3 | Theoretical investigation

Complete-active-space self-consistent field (CASSCF) calculations on individual Dy<sup>III</sup> or Ho<sup>III</sup> fragment in complexes 3 and 4 based on X-ray-determined geometries have been carried out with MOLCAS 8.2<sup>[36]</sup> and SINGLE\_ANISO<sup>[37]</sup> programs. Binuclear complexes 3 and 4 with central symmetrical structure have one type of magnetic center Dy<sup>III</sup> and Ho<sup>III</sup> ion, respectively. CASSCF calculations on individual Dy<sup>III</sup> or Ho<sup>III</sup> fragment for 3 and 4 (see Figure 11 for the calculated model structures of 3 and 4) based on single-crystal X-ray-determined geometry have been carried out with MOLCAS 8.2<sup>[36]</sup> program package. Each individual Dy<sup>III</sup> or Ho<sup>III</sup> fragment

**TABLE 1** Differences in structural and magnetic parameters between complex **3** and the reported pure Salen-type Dy<sub>2</sub> SMMs

| Molecular formula  | Coordination mode                | Bond distance/Å |                            |  | Reference           |
|--|----------------------------------|-----------------|----------------------------|--|---------------------|
|  |                                  | Dy···Dy         | <i>U</i> <sub>eff</sub> /K |  |                     |
| [Dy <sub>2</sub> (L) <sub>2</sub> (MeOH) <sub>2</sub> (NO <sub>3</sub> ) <sub>2</sub><br>HL = <i>N,N'</i> -bis(5-bromosalicylidene)<br>ethane-1,2-diamine  | N <sub>2</sub> O <sub>6</sub>    | 3.816           | 47.68                      |  | This work           |
| [Dy(H <sub>2</sub> L)(OAc) <sub>2</sub> ] <sub>2</sub> (PF <sub>6</sub> ) <sub>2</sub> ·4CH <sub>2</sub> Cl <sub>2</sub> H <sub>2</sub> L = <i>N,N'</i> -bis(2-hydroxy-3-methoxybenzylidene)-1,3-propanediamine  | O <sub>9</sub>                   | 3.807           | 28                         |  | [26d]               |
| [Dy(H <sub>2</sub> L) <sub>2</sub> (NO <sub>3</sub> ) <sub>2</sub> ] <sub>2</sub> (PF <sub>6</sub> ) <sub>4</sub> ·4CH <sub>2</sub> Cl <sub>2</sub> ·0.5C <sub>6</sub> H <sub>14</sub> H <sub>2</sub> L <sup>1</sup> = <i>N,N'</i> -bis(salicylidene)-1,3-propanediamine | O <sub>9</sub> , O <sub>10</sub> | 3.840           | 32.5                       |  | [26d]               |
| [Dy <sub>2</sub> (valdien) <sub>2</sub> (ClCH <sub>2</sub> OO) <sub>2</sub> ] Hvaldien = <i>N<sub>1</sub>,N<sub>3</sub></i> -bis(3-methoxysalicylidene)diethylenetriamine  | N <sub>3</sub> O <sub>5</sub>    | 3.798           | 50                         |  | [13a]               |
| [Dy <sub>2</sub> (valdien) <sub>2</sub> (Cl <sub>2</sub> CHCOO) <sub>2</sub> ] <sub>2</sub> ·0.5CH <sub>2</sub> OH Hvaldien = <i>N<sub>1</sub>,N<sub>3</sub></i> -bis(3-methoxysalicylidene)diethylenetriamine   | N <sub>3</sub> O <sub>5</sub>    | 3.796           | 60                         |  | [13a]               |
| [Dy <sub>2</sub> (valdien) <sub>2</sub> (CH <sub>3</sub> COCHCOCH <sub>3</sub> ) <sub>2</sub> ] <sub>2</sub> ·2CH <sub>2</sub> Cl <sub>2</sub> Hvaldien = <i>N<sub>1</sub>,N<sub>3</sub></i> -bis(3-methoxysalicylidene)diethylenetriamine                               | N <sub>3</sub> O <sub>5</sub>    | 3.895           | 16                         |  | [13a]               |
| [Dy <sub>2</sub> (valdien) <sub>2</sub> ](CF <sub>3</sub> COCHCOFC <sub>3</sub> ) <sub>2</sub> ] H <sub>2</sub> valdien = <i>N<sub>1</sub>,N<sub>3</sub></i> -bis(3-methoxysalicylidene)diethylenetriamine   | N <sub>3</sub> O <sub>5</sub>    | 3.835           | 110                        |  | [13a]               |
| [Dy <sub>2</sub> (valdien) <sub>2</sub> (NO <sub>3</sub> ) <sub>2</sub> ] Hvaldien = <i>N<sub>1</sub>,N<sub>3</sub></i> -bis(3-methoxysalicylidene)diethylenetriamine  | N <sub>3</sub> O <sub>5</sub>    | 3.768           | 76                         |  | [34b <sup>1</sup> ] |

in **3** and **4** was calculated by keeping the experimentally determined structure of the corresponding compound while replacing the neighboring Dy<sup>III</sup> or Ho<sup>III</sup> ion by diamagnetic Lu<sup>III</sup>. The energy levels (cm<sup>-1</sup>), g (g<sub>x</sub>, g<sub>y</sub>, g<sub>z</sub>) tensors, and the predominant *m<sub>J</sub>* values of the lowest eight or nine spin-orbit states of individual Dy<sup>III</sup> or Ho<sup>III</sup> fragment for **3** and **4** are presented in **Table S4**. The *m<sub>J</sub>* components for the lowest two Kramers doublets (KD)s of individual Dy<sup>III</sup> or Ho<sup>III</sup> fragment for **3** and **4** are shown in **Table S5**, where the ground KD for Dy<sup>III</sup> is mostly composed by *m<sub>J</sub> = ±15/2*, and its first excited state is mostly composed by *m<sub>J</sub> = ±13*. However, the ground non-KD for Ho<sup>III</sup> is mostly composed by *m<sub>J</sub> = ±8*, and the first excited state is composed by several *m<sub>J</sub>* states severely. The corresponding magnetization blocking barriers of individual Dy<sup>III</sup> or Ho<sup>III</sup> fragment for **3** and **4** are shown in Figure 12, where the transversal magnetic moment in the ground state of individual Dy<sup>III</sup> fragment in **3** is  $0.24 \times 10^{-2} \mu_B$ , and thus the QTM in its ground KD could be suppressed at low temperature. The energy differences between the ground and the first excited state for individual Dy<sup>III</sup> fragment of complex **3** is 189 cm<sup>-1</sup> (271.9 K), which is larger than its experimental energy barrier of 47.68 K, which can be correlated with the QTM effect and other relaxation process.<sup>[38]</sup> However, the transversal magnetic moment in the ground state of individual Ho<sup>III</sup> fragment for **4** is  $0.27 \mu_B$ , thus allowing a fast QTM in its ground state, which is likely to show weak SMM characteristics as also visible in our AC-

susceptibility studies (absence of clear maxima in the  $\chi''$  peak for complex **4**). Although their magnetic anisotropies mainly come from individual Dy<sup>III</sup> or Ho<sup>III</sup> ions, the Dy<sup>III</sup>-Dy<sup>III</sup> or Ho<sup>III</sup>-Ho<sup>III</sup> interactions have some certain influence on their slow magnetic relaxation processes.

The calculated ground g<sub>z</sub> values of individual Dy<sup>III</sup> or Ho<sup>III</sup> fragment in complexes **3** and **4** are close to 20, which shows that the Dy<sup>III</sup>-Dy<sup>III</sup> or Ho<sup>III</sup>-Ho<sup>III</sup> exchange interaction can be approximately regarded as the Ising type. The program POLY\_ANISO<sup>[37]</sup> was used to fit the magnetic susceptibilities of complexes **3** and **4** using the total parameters from Table 2. For **1**, the magnetic interaction between two Gd<sup>III</sup> ions is isotropic. The program POLY\_ANISO was also used to fit the total magnetic interaction

**TABLE 2** Fitted exchange couplings *J*<sup>%</sup><sub>exch</sub>, the calculated dipole-dipole interactions *J*<sup>%</sup><sub>dip</sub>, and the total constants *J*<sup>%</sup><sub>total</sub> between magnetic center ions in **3** and **4** (cm<sup>-1</sup>), and the total isotropic magnetic interaction parameter of *J*<sub>total</sub> in 1 (cm<sup>-1</sup>). The intermolecular interactions z*J* of **1**, **3**, and **4** were fitted to -0.05, -0.09, and -0.01 cm<sup>-1</sup>, respectively

|  | <b>1</b> | <b>3</b> | <b>4</b> |
|--|----------|----------|----------|
| <i>J</i> <sup>%</sup> <sub>dip</sub>   |          | 0.85     | 0.73     |
| <i>J</i> <sup>%</sup> <sub>exch</sub>  |          | -3.00    | -2.08    |
| <i>J</i> <sup>%</sup> <sub>total</sub> |          | -2.15    | -1.35    |
| <i>J</i> <sub>total</sub>              | -0.25    |          |          |

parameter of  $J$  through comparison of the computed and measured magnetic susceptibility.

The parameters from Table 2 were calculated with respect to the pseudospin  $S_{Dy}^{\%} = 1/2$  of the Dy<sup>III</sup> ion, the pseudospin  $S_{Ho}^{\%} = 1/2$  of the Ho<sup>III</sup> ion, and the spin  $S_{Gd} = 7/2$  of the Gd<sup>III</sup> ion. For **3** and **4**, the dipolar magnetic coupling constants  $J_{\text{dip}}^{\%}$  were calculated exactly, whereas the exchange coupling constants  $J_{\text{exch}}^{\%}$  were fitted through comparison of the computed and measured magnetic susceptibilities using the POLY\_ANISO program. For **1**, the total isotropic magnetic interaction parameter of  $J_{\text{total}}$  was included to fit the magnetic susceptibilities. The calculated and experimental  $\chi_M T$  versus  $T$  plots of complexes **1**, **3**, and **4** are shown in Figure 3, where their fits are close to the experiments.<sup>[39]</sup> From Table 2, the Dy<sup>III</sup>-Dy<sup>III</sup> and Ho<sup>III</sup>-Ho<sup>III</sup> interactions in **3** and **4** within the Lines model<sup>[40]</sup> are both antiferromagnetic. We gave the exchange energies, the energy differences between each exchange doublet  $\Delta_t$ , and the main values of the  $g_z$  for the lowest two exchange doublets of **1**, **3**, and **4** in Table S6, where the  $g_z$  values of the ground exchange states for **1**, **3**, and **4** are all close to 0.000, which confirms that the Gd<sup>III</sup>-Gd<sup>III</sup>, Dy<sup>III</sup>-Dy<sup>III</sup>, and Ho<sup>III</sup>-Ho<sup>III</sup> interactions for **1**, **3**, and **4** are all antiferromagnetic. In addition, based on structural data, the shortest intermolecular Ln<sup>III</sup>-Ln<sup>III</sup> distance is about 7.0690(18), 7.0824(14), 7.0984(10) Å for complexes **1**, **3**, and **4**, respectively, which may produce intermolecular dipole-dipole interactions. The main magnetic axes on two Dy<sup>III</sup> or Ho<sup>III</sup> ions of **3** and **4** indicated in Figure S13 are both antiparallel).

## 4 | CONCLUSIONS

In summary, a series of dinuclear lanthanide complexes based on the Salen-type ligand, *N,N'*-bis(5-bromosalicylidene)ethane-1,2-diamine ( $H_2L$ ), were synthesized by the solvothermal method in this work. Magnetic studies show that the [Dy<sub>2</sub>] complex behaves as a zero-field SMM with an anisotropy barrier of  $U_{\text{eff}} \approx 47.68$ , exhibiting a comparatively higher  $U_{\text{eff}}$  among the pure Salen-type dinuclear dysprosium SMMs. The [Ho<sub>2</sub>] complex is a rare phenoxy-O-bridged Ho<sub>2</sub>-Salen-type complex with slow magnetic relaxation behavior. *Ab initio* calculations and fitting of the magnetic susceptibilities indicate the existence of antiferromagnetic Ln<sup>III</sup>-Ln<sup>III</sup> interactions in the phenoxy-O-bridged binuclear Ln<sup>III</sup> compounds. The obtained result in this contribution enriches the pure polynuclear lanthanide Salen chemistry, and moreover, our work encourages researchers to further explore similar structures by

modifying ligands and to investigate the magneto-structural relationship in depth.

## ACKNOWLEDGEMENTS

This work was supported by the Foundation for Young Talents in College of Anhui Province (no. gxyqZD2016412), the Anhui Provincial Innovation Team of Design and Application of Advanced Energetic Materials (KJ2015TD003).

## FUNDING INFORMATION

Foundation for Young Talents in College of Anhui Province (no. gxyqZD2016412), Anhui Provincial Innovation Team of Design and Application of Advanced Energetic Materials (KJ2015TD003).

## ORCID

Pei-Pei Yang  <https://orcid.org/0000-0002-7095-3195>

## REFERENCES

- [1] a)E. Saitoh, H. Miyajima, T. Yamaoka, G. Tatara, *Nature* **2004**, 432, 203. b)L. Bogani, W. Wernsdorfer, *Nat. Mater.* **2008**, 7, 179. c)T. F. Zheng, S. L. Yao, C. Cao, S. J. Liu, H. K. Hu, T. Zhang, H. P. Huang, J. S. Liao, J. L. Chena, H. R. Wen, *New J. Chem.* **2017**, 41, 8598.
- [2] a)R. Sessoli, A. K. Powell, *Coord. Chem. Rev.* **2009**, 253, 2328. b)L. Sorace, C. Benelli, D. Gatteschi, *Chem. Soc. Rev.* **2011**, 40, 3092. c)H. L. C. Feltham, S. Brooker, *Coord. Chem. Rev.* **2014**, 276, 1.
- [3] N. Ishikawa, M. Sugita, T. Ishikawa, S. Y. Koshihara, Y. Kaizu, *J. Am. Chem. Soc.* **2003**, 125, 8694.
- [4] a)D. N. Woodruff, R. E. P. Winpenny, R. A. Layfield, *Chem. Rev.* **2013**, 113, 5110. b)S. T. Liddle, J. van Slageren, *Chem. Soc. Rev.* **2015**, 44, 6655.
- [5] a)D. Gatteschi, *Nat. Chem.* **2011**, 3, 830. b)J. Luzon, R. Sessoli, *Dalton Trans.* **2012**, 41, 13556.
- [6] a)Y. N. Guo, G. F. Xu, Y. Guo, J. Tang, *Dalton Trans.* **2011**, 40, 9953. b)J. D. Rinehartand, J. R. Long, *Chem. Sci.* **2011**, 2, 2078. c) K. Liu, X. Zhang, X. Meng, W. Shi, P. Chengab, A. K. Powell, *Chem. Soc. Rev.* **2016**, 45, 2423. d) C. A. P. Goodwin, F. Ortú, D. Reta, N. F. Chilton, D. P. Mills, *Nature* **2017**, 548, 439.
- [7] S. Ghosh, S. Mandal, M. K. Singh, C. M. Liu, G. Rajaraman, S. Mohanta, *Dalton Trans.* **2018**, 47, 11455.
- [8] F. S. Guo, B. M. Day, Y.-C. Chen, M. L. Tong, A. Mansikkämäki, R. A. Layfield, *Science* **2018**, 362, 1400.
- [9] J. P. Costes, F. Dahan, A. Dupuis, *Inorg. Chem.* **2000**, 39, 165.
- [10] a)L. E. Roy, T. Hughbanks, *J. Am. Chem. Soc.* **2006**, 128, 568. b)G. Rajaraman, F. Totti, A. Bencini, A. Caneschi, R. Sessoli, D. Gatteschi, *Dalton Trans.* **2009**, 17, 3153. c)S. K. Singh, N. K. Tibrewal, G. Rajaraman, *Dalton Trans.* **2011**, 40, 10897. d)T. Rajeshkumar, G. Rajaraman, *Chem. Commun.* **2012**, 48, 7856. e)M. K. Singh, T. Rajeshkumar, R. Kumar, S. K. Singh, G. Rajaraman, *Inorg. Chem.* **2018**, 57, 1846.
- [11] K. Zhang, D. Liu, V. Vieru, L. Hou, B. Cui, F. S. Guo, L. F. Chibotaru, Y. Y. Wang, *Dalton Trans.* **2017**, 46, 638.

- [12] a)Z. Chen, Y. H. Lan, C. L. Su, Y. Q. Zhang, W. Wernsdorfer, *Dalton Trans.* **2018**, *47*, 15298. b)S. Biswas, P. Kumar, A. Swain, T. Gupta, P. Kalita, S. Kundu, G. Rajaraman, V. Chandrasekhar, *Dalton Trans.* **2019**, *48*, 6421. c)J. T. Coutinho, C. C. L. Pereira, J. Marçalo, J. J. Baldoví, M. Almeida, B. Monteiro, L. C. J. Pereira, *Dalton Trans.* **2018**, *47*, 16211. d)I. F. Díaz-Orteg, J. M. Herrera, T. Gupta, G. Rajaraman, H. Nojiri, E. Colacio, *Inorg. Chem.* **2017**, *56*, 5594.
- [13] a) E. C. Mazarakioti, J. Regier, L. Cunha-Silva, W. Wernsdorfer, M. Pilkington, J. K. Tang, T. C. Stamatatos, *Inorg. Chem.* **2017**, *56*, 3568. b) Z. X. Xiao, H. Miao, D. Shao, H. Y. Wei, Y. Q. Zhang, X. Y. Wang, *Dalton Trans.* **2018**, *47*, 7925. c)S. Yu, Z. B. Hu, Z. L. Chen, B. Li, Y. Q. Zhang, Y. N. Liang, D. C. Liu, D. Yao, F. P. Liang, *Inorg. Chem.* **2019**, *58*, 1191.
- [14] R. P. Li, Q. Y. Liu, Y. L. Wang, C. M. Liu, S. J. Liu, *Inorg. Chem. Front.* **2017**, *4*, 1149.
- [15] a)V. Chandrasekhar, S. Hossain, S. Das, S. Biswas, J. P. Sutter, *Inorg. Chem.* **2013**, *52*, 6346. b)K. Zhang, G. P. Li, V. Montigaud, O. Cadot, B. L. Guennic, J. K. Tang, Y. Y. Wang, *Dalton Trans.* **2019**, *48*, 2135.
- [16] a)G. J. Chen, C. Y. Gao, J. L. Tian, J. K. Tang, W. Gu, X. Liu, S. P. Yan, D. Z. Liao, P. Cheng, *Dalton Trans.* **2011**, *40*, 5579. b)P. Zhang, L. Zhang, C. Wang, S. Xue, S. Y. Lin, J. Tang, *J. Am. Chem. Soc.* **2014**, *136*, 4484. c)C. Wang, S. Y. Lin, J. F. Wu, S. W. Yuan, J. K. Tang, *Dalton Trans.* **2015**, *44*, 4648.
- [17] S. F. Xue, L. Zhao, Y. N. Guo, J. K. Tang, *Dalton Trans.* **2012**, *41*, 351.
- [18] a)A. Watanabe, A. Yamashita, M. Nakano, T. Yamamura, T. Kajiwara, *Chem.-Eur. J.* **2011**, *17*, 7428. b)T. Hamamatsu, K. Yabe, M. Towatari, S. Osa, N. Matsumoto, N. Re, A. Pochaba, J. Mrozinski, J. L. Gallani, A. Barla, P. Imperia, C. Paulsen, J. P. Kappler, *Inorg. Chem.* **2007**, *46*, 4458. c)M. X. Yao, Q. Zheng, F. Gao, Y. Z. Li, Y. Song, J. L. Zuo, *Dalton Trans.* **2012**, *41*, 13682. d)X. C. Huang, C. Zhou, H. Y. Wei, X. Y. Wang, *Inorg. Chem.* **2013**, *52*, 7314. e)J. Long, J. Rouquette, J. M. Thibaud, R. A. S. Ferreira, L. D. Carlos, B. Donnadieu, V. Vieru, L. F. Chibotaru, L. Konczewicz, J. Haines, Y. Guari, J. Larionova, *Angew. Chem. Int. Ed.* **2015**, *54*, 2236.
- [19] a)F. Luan, T. Q. Liu, P. F. Yan, X. Y. Zou, Y. X. Li, G. M. Li, *Inorg. Chem.* **2015**, *54*, 3485. b)P. H. Lin, W. B. Sun, M. F. Yu, G. M. Li, P. F. Yan, M. Murugesu, *Chem. Commun.* **2011**, *47*, 10993. c)Y. M. Yue, P. F. Yan, J. W. Sun, G. M. Li, *Inorg. Chem. Comm.* **2015**, *54*, 5. d)W. Y. Zhang, P. Chen, Y. M. Tian, H. F. Li, W. B. Sun, P. F. Yan, *CrystEngComm* **2018**, *20*, 777. e)Z. Y. Liu, H. H. Zou, R. Wang, M. S. Chen, F. P. Liang, *RSC Adv.* **2018**, *8*, 767. f) T. Q. Liu, P. F. Yan, F. Luan, Y. X. Li, J. W. Sun, C. C. Fan, Y. H. Chen, X. Y. Zou, G. M. Li, *Inorg. Chem.* **2015**, *54*, 221. g)J. Zhu, H. F. Song, P. F. Yan, G. F. Houa, G. M. Li, *CrystEngComm* **2013**, *15*, 1747.
- [20] D. F. Wu, H. Y. Shen, X. Y. Chu, W. J. Chang, L. H. Zhao, Y. Y. Duan, H. H. Chen, J. Z. Cui, H. L. Gao, *New J. Chem.* **2018**, *42*, 16836.
- [21] G. M. Sheldrick, University of Göttingen. **2002**.
- [22] a)S. Jana, P. P. Jana, S. Chattopadhyay, *J. Coord. Chem.* **2015**, *14*, 2520. b)Y. Z. Zheng, Y. Lan, C. E. Anson, A. K. Powell, *Inorg. Chem.* **2008**, *47*, 10813.
- [23] M. S. Kumar, M. Schwidder, W. Grünert, U. Bentrup, A. Brückner, *J. Catal.* **2006**, *239*, 173.
- [24] K. Liu, X. J. Zhang, X. X. Meng, W. Shi, P. Cheng, A. K. Powell, *Chem. Soc. Rev.* **2016**, *45*, 2423.
- [25] M. Llunell, D. Casanova, J. Cirera, P. Alemany, S. Alvarez, *SHAPE, version 2.1*, Universitat de Barcelona, Barcelona, Spain **2013**.
- [26] a)H. D. Li, J. Sun, M. Yang, Z. Sun, J. K. Tang, Y. Ma, L. C. Li, *Inorg. Chem.* **2018**, *57*, 9757. b)H. Y. J. X. Yang, J. Q. Han, P. F. Li, Y. L. Hou, W. M. Wang, M. Fang, *New J. Chem.* **2019**, *43*, 8067. c)X. Y. Zou, P. F. Yan, Y. P. Dong, F. Luana, G. M. Li, *RSC Adv.* **2015**, *5*, 96573. d)X. Y. Zou, Y. P. Dong, F. M. Zhang, G. M. Li, *Inorg. Chim. Acta* **2018**, *473*, 37.
- [27] W. Sethi, S. Sanz, K. S. Pedersen, M. A. Sørensen, G. S. Nichol, G. Lorusso, M. Evangelisti, E. K. Brechin, S. Piligkos, *DaltonTrans.* **2015**, *44*, 10315.
- [28] C. Bai, C. T. Li, H. M. Hu, B. Liu, J. D. Li, G. I. Xue, *Dalton Trans.* **2019**, *48*, 814.
- [29] a)S. J. Liu, C. Cao, C. C. Xie, T. F. Zheng, X. L. Tong, J. S. Liao, J. L. Chen, H. R. Wen, Z. Chang, X. H. Bu, *Dalton Trans.* **2016**, *45*, 9209. b)G. Novitchi, W. Wernsdorfer, L. F. Chibotaru, J. P. Costes, C. E. Anson, A. K. Powell, *Angew. Chem. Int. Ed.* **2009**, *48*, 1614.
- [30] a)F. Gao, X. Feng, L. Yang, X. Chen, *DaltonTrans.* **2016**, *45*, 7476. b)F. Gao, F. L. Yang, G. Z. Zhu, Y. Zhao, *DaltonTrans.* **2015**, *44*, 20230. c)A. J. Hutchings, F. Habib, R. J. Holmberg, I. Korobkov, M. Murugesu, *Inorg. Chem.* **2014**, *53*, 2102.
- [31] a)H. Zhu, S. Li, C. Gao, X. Xiong, Y. Zhang, L. Liu, A. K. Powell, S. Gao, *DaltonTrans.* **2016**, *45*, 4614. b)F. Wu, L. Zhao, L. Zhang, X. L. Li, M. Guo, A. K. Powell, J. K. Tang, *Angew. Chem. Int. Ed.* **2016**, *55*, 15574. c)Y. Ge, Z. Y. Chen, H. Y. Wang, H. Wang, P. Wang, X. Duana, D. X. Huo, *New J. Chem.* **2018**, *42*, 17968.
- [32] Y. Gao, G. Xu, L. Zhao, J. K. Tang, Z. Liu, *Inorg. Chem.* **2009**, *48*, 1148.
- [33] Y. Katoh, N. Horii, W. Yasuda, K. Wernsdorfer, B. K. Toriumi, B. K. Breedlove, M. Yamashita, *DaltonTrans* **2012**, *41*, 13582.
- [34] a)F. Habib, G. Brunet, V. Vieru, I. Korobkov, L. F. Chibotaru, M. Murugesu, *J. Am. Chem. Soc.* **2013**, *135*, 13242. b)J. Long, F. Habib, P. H. Lin, I. Korobkov, G. Enright, L. Ungur, W. F. Wernsdorfer, L. F. Chibotaru, M. Murugesu, *J. Am. Chem. Soc.* **2011**, *133*, 5319.
- [35] J. Zhang, H. F. Zhang, Y. M. Chen, X. F. Zhang, Y. H. Li, W. Liu, Y. P. Dong, *DaltonTrans.* **2016**, *45*, 16463.
- [36] F. Aquilante, J. Autschbach, R. K. Carlson, L. F. Chibotaru, M. G. Delcay, L. De Vico, I. Fdez. Galván, N. Ferré, L. M. Frutos, L. Gagliardi, M. Garavelli, A. Giussani, C. E. Hoyer, G. L. Manni, H. Lischka, D. Ma, P. Å. Malmqvist, T. Müller, A. Nenov, M. Olivucci, T. B. Pedersen, D. Peng, F. Plasser, B. Pritchard, M. Reiher, I. Rivalta, I. Schapiro, J. Segarra-Martí, M. Stenrup, D. G. Truhlar, L. Ungur, A. Valentini, S. Vancoillie, V. Veryazov, V. P. Vysotskiy, O. Weingart, F. Zapata, R. Lindh, *J. Comput. Chem.* **2016**, *37*, 506.
- [37] a) L. F. Chibotaru, L. Ungur, A. Soncini, *Angew. Chem. Int. Ed.* **2008**, *47*, 4126. b) L. Ungur, W. Van den Heuvel, L. F. Chibotaru, *New J. Chem.* **2009**, *33*, 1224. c)L. F. Chibotaru, L. Ungur, C. Aronica, H. Elmoll, G. Pilet, D. Luneau, *J. Am. Chem. Soc.* **2008**, *130*, 12445.

- [38] K. R. Vignesh, S. K. Langley, K. S. Murray, G. Rajaraman, *Inorg. Chem.* **2017**, *56*, 2518.
- [39] S. K. Langley, D. P. Wielechowski, V. Vieru, N. F. Chilton, B. Moubaraki, B. F. Abrahams, L. F. Chibotaru, K. S. Murray, *Angew. Chem. Int. Ed.* **2013**, *52*, 12014.
- [40] M. E. Lines, *J. Chem. Phys.* **1971**, *55*, 2977.

## SUPPORTING INFORMATION

Additional supporting information may be found online in the Supporting Information section at the end of this article.

**How to cite this article:** Zhang L, Yang P-P, Li L-F, Hu Y-Y, Gao Y, Tao J. A series of Salen-type homodinuclear lanthanide complexes and their slow magnetic relaxation in Dy<sub>2</sub> and Ho<sub>2</sub>. *Appl Organometal Chem.* 2020;e5331. <https://doi.org/10.1002/aoc.5331>